

DOI:10.20135/j.issn.1006-8147.2024.05.0415

论著

探讨血必净注射液治疗重症急性胰腺炎肺损伤的机制

王舜¹,张桂贤²,冯志乔³,沈洪昇²,李文畅²,宗文辉²,蔡隽²,刘洪斌²

(1.天津医科大学研究生院,天津300070;2.天津市医药科学研究所,天津300020;3.天津红日药业股份有限公司,天津301700)

摘要 目的:探讨血必净(XBJ)注射液对重症急性胰腺炎(SAP)大鼠肺损伤模型的治疗机制。方法:将80只雄性Sprague-Dawley(SD)大鼠随机分为4组:对照组、SAP模型组、XBJ低剂量治疗组、XBJ高剂量治疗组,每组20只。除对照组,各组大鼠均经胰胆管匀速逆行注射4.5%牛磺胆酸钠溶液(0.1 mL/100 g,0.05 mL/min)以诱发SAP,造模成功30 min后,将XBJ低、高剂量治疗组大鼠经尾静脉注射XBJ(剂量分别为5、20 mL/kg),对照组及模型组给予等体积生理盐水。24 h后,从每组中随机抽取10只大鼠,经尾静脉注射Evans blue检测肺组织毛细血管通透性。处死余下的各组大鼠,取腹水测量其体积;取部分胰腺及肺组织计算组织干湿重比值;苏木精-伊红(HE)染色观察胰腺、肺脏的病理改变,并进行病理评分;酶联免疫吸附法(ELISA)检测腹水淀粉酶含量;Western印迹法检测肺组织中ROCK1、MYPT1、pMLC的相对表达量。结果:SAP模型组较对照组腹水量及腹水淀粉酶含量明显升高($t=-21.73$ 、 -40.72 ,均 $P<0.01$);SAP模型组、XBJ低剂量组、XBJ高剂量组腹水量及腹水淀粉酶含量逐渐降低($F=39.66$ 、 141.78 ,均 $P<0.01$)。SAP模型组较对照组,胰腺干湿重比值、肺脏干湿重比值明显降低($t=19.83$ 、 15.47 ,均 $P<0.01$),肺组织中Evans blue渗出量明显增高($t=-27.9$, $P<0.01$);SAP模型组、XBJ低剂量组、XBJ高剂量组胰腺干湿重比值、肺脏干湿重比值逐渐升高($F=75.19$ 、 15.47 ,均 $P<0.01$),肺组织中Evans blue渗出量逐渐降低($F=99.52$, $P<0.01$)。对照组大鼠胰腺组织结构完整,SAP模型组大鼠胰腺病理得分明显升高($t=-42.79$, $P<0.01$);XBJ低剂量组、XBJ高剂量组大鼠胰腺病理得分逐渐降低($F=175.43$, $P<0.01$)。对照组大鼠肺组织结构完整,SAP模型组大鼠病理得分明显升高($t=-37.57$, $P<0.01$);XBJ低剂量组、XBJ高剂量组大鼠肺组织病变减轻,病理得分逐渐降低($F=126.00$, $P<0.01$)。SAP模型组较对照组肺组织中ROCK1、pMLC蛋白表达量明显升高($t=-16.97$ 、 -13.53 ,均 $P<0.01$),MYPT1表达量显著降低($t=23.30$, $P<0.01$);SAP模型组、XBJ低剂量组、XBJ高剂量组肺组织中ROCK1、pMLC蛋白表达量逐渐降低($F=84.89$ 、 50.84 ,均 $P<0.01$),MYPT1表达量显著升高($F=48.68$, $P<0.01$)。结论:XBJ通过降低多种细胞因子及DAMPs形成,抑制ROCK1-MYPT1-pMLC信号通路活化,对SAP肺损伤起到治疗的作用。

关键词 重症急性胰腺炎;急性肺损伤;血必净注射液

中图分类号 R285.5

文献标志码 A

文章编号 1006-8147(2024)05-0415-07

Study on the mechanism of Xuebijing injection in treating severe acute pancreatitis with lung injury

WANG Shun¹,ZHANG Guixian²,FENG Zhiqiao³,SHEN Hongsheng²,LI Wenchang²,ZONG Wenhui²,CAI Jun²,LIU Hongbin²

(1.Graduate School of Tianjin Medical University,Tianjin 300070,China;2.Tianjin Institute of Medical & Pharmaceutical Sciences,Tianjin 300020,China;3.Tianjin Chase Sun Pharmaceutical Co.,Ltd. Tianjin 301700,China)

Abstract Objective: To investigate the therapeutic mechanism of Xuebijing(XBJ) injection on lung injury model of severe acute pancreatitis(SAP) in rats. **Methods:** A total of 80 male Spruce Dawley(SD) rats were randomly divided into 4 groups: control group, SAP model group, XBJ low-dose treatment group and XBJ high-dose treatment group, with 20 rats in each group. Except for the control group, the rats in all groups were injected with 4.5% sodium taurocholate solution(0.1 mL/100 g,0.05 mL/min) at uniform speed retrograde through the pancreatic bile duct to induce SAP. 30 min after successful molding, the rats in the low-dose and high-dose XBJ treatment groups were injected with XBJ injection through the tail vein(the dose was 5 and 20 mL/kg, respectively). Control group and model group were given equal volume normal saline. After 24 h, 10 rats were randomly selected from each group, and Evans blue was injected into the tail vein to detect the capillary permeability of lung tissue. The remaining rats were killed and their volume was measured with ascites. The dry-wet weight ratio was calculated by taking part of pancreas and lung tissues. Hematoxylin-eosin(HE) staining was used to observe the pathological changes of pancreas and lung, and pathological score was performed. The amylase content of ascites was detected by enzyme-linked immunosorbent assay(ELISA). The relative expression levels of ROCK1,MYPT1 and pMLC in lung tissues were detected by Western blotting. **Results:** Compared with the control group, the water volume and amylase content of ascites in SAP model group were significantly increased ($t=-21.73$ 、 -40.72 , both $P<0.01$). Compared with SAP model group, XBJ low-dose

基金项目 天津市科技计划项目(21JCZDJC01220);国家自然科学基金项目(82304797);天津市科技计划项目(21JCYBJC01680);天津市卫生健康科技项目(TJWJ2022MS049)

作者简介 王舜(1994-),男,主治医师,硕士在读,研究方向:中西医结合防治重症急性胰腺炎;通信作者:刘洪斌,E-mail:jtss@sina.com。

group and XBJ high-dose group, the water volume and amylase content of ascites gradually decreased ($F=39.66, 141.78$, both $P<0.01$). Compared with the control group, the dry-wet weight ratio of pancreas and dry-wet weight ratio of lung were significantly decreased in SAP model group ($t=19.83, 15.47$, both $P<0.01$), and the Evans blue exudation amount in lung tissue was significantly increased ($t=-27.9, P<0.01$). Compared with SAP model group, XBJ low-dose group and XBJ high-dose group, the dry-wet weight ratio of pancreas and dry-wet weight ratio of lung were gradually increased ($F=75.19, 15.47$, both $P<0.01$), and the Evans blue exudation amount in lung tissue was gradually decreased ($F=99.52, P<0.01$). The pancreatic tissue structure of the control group was intact, and the pancreatic pathological score of the SAP model group was significantly increased ($t=-42.79, P<0.01$). The pathological scores of the pancreas in the low-dose group and the high-dose group of XBJ decreased gradually ($F=175.43, P<0.01$). The lung structure of the control group was intact, and the pathological score of the SAP model group was significantly increased ($t=-37.57, P<0.01$). Compared with the low-dose group of XBJ and the high-dose group of XBJ, the lung tissue lesions were reduced, and the pathological scores were decreased gradually ($F=126.00, P<0.01$). Compared with the control group, the expression levels of ROCK1 and pMLC protein in SAP model group were significantly increased ($t=-16.97, -13.53$, both $P<0.01$), and the expression level of MYPT1 was significantly decreased ($t=23.30, P<0.01$). Compared with SAP model group, XBJ low-dose group and XBJ high-dose group, the expression levels of ROCK1 and pMLC protein in lung tissue gradually decreased ($F=84.89, 50.84$, both $P<0.01$), while the expression levels of MYPT1 were significantly increased ($F=48.68, P<0.01$). **Conclusion:** XBJ plays a therapeutic role in SAP lung injury by reducing the formation of various cytokines and DAMPs, inhibiting the activation of ROCK1-MYPT1-pMLC signaling pathway.

Key words severe acute pancreatitis; acute lung injury; Xuebijing injection

急性胰腺炎(acute pancreatitis, AP)合并急性肺损伤/急性呼吸窘迫综合征(ALI/ARDS)时为重症急性胰腺炎(severe acute pancreatitis, SAP)^[1]。SAP的病死率高,是当下危重医学领域重点的研究方向^[2-3]。AP早期,由于胰酶的异常激活导致胰腺及周围组织急性炎症,引发细胞因子激增、损伤相关的分子模式(DAMPs)大量释放等造成系统性炎症反应综合征(systemic inflammatory response syndrome, SIRS),可直接引发ALI/ARDS的形成^[4-7]。ALI/ARDS的病理基础为弥漫性肺泡-毛细血管损伤,病情初期表现为毛细血管通透性的持续升高^[8-9]。

Rho相关卷曲包含蛋白激酶1(ROCK1),可抑制肌球蛋白磷酸酶靶亚基1(MYPT1)的表达,使肌球蛋白轻链(MLC)磷酸化形成pMLC,参与细胞骨架变构、收缩、黏附和迁移等生理过程,并且在调节毛细血管内皮细胞通透性中起重要作用^[10-12]。血必净注射液(Xuebijing Injection, XBJ)可以显著改善SIRS、多器官功能衰竭综合征(multiple organ dysfunction syndrome, MODS)的预后,多项实验研究已证实其在SAP治疗中的效果显著^[13-16],但具体机制尚未阐明。本研究通过制备SAP大鼠肺损伤模型,基于ROCK1-MYPT1-pMLC信号通路及毛细血管通透性的变化来探讨XBJ的治疗机制。

1 材料与方法

1.1 材料与试剂

1.1.1 实验动物 SPF级雄性Sprague-Dawley(SD)大鼠80只[许可证号:SCXK(京)2021-0011,北京维通利华],质量250~300 g,本实验经天津市医药科学研究所动物实验伦理委员会审批,批准号

S21DYZD3097。

1.1.2 主要试剂及仪器 XBJ(天津红日药业,生产批号2212011);牛磺胆酸钠(Sigma);低温高速离心机(Eppendorf);化学发光分析仪(Tanon-5200);垂直电泳系统(Bio-Rad);CX41微图HTC1600正置显微镜(Olympus);大鼠淀粉酶检测试剂盒(盖德化工);BCA蛋白质定量试剂盒(Thermo Fisher Scientific);ROCK1抗体、MYPT1抗体、pMLC抗体(BOSTER),GAPDH抗体(优抗),羊抗兔IgG-HRP、羊抗鼠IgG-HRP(Affinity);DAB显色试剂盒(北京中杉金桥)。

1.2 方法

1.2.1 实验分组及模型制备 雄性SD大鼠随机分为4组,分别为对照组、SAP模型组、XBJ低剂量治疗组、XBJ高剂量治疗组,每组20只。除对照组,予4.5%牛磺胆酸钠0.1 mL/100 g,以0.05 mL/min匀速泵入大鼠胰胆管内,制备SAP大鼠模型,观察到胰腺组织局部逐渐出现暗红色、水肿以及渗出改变时,表明SAP大鼠模型制备成功。XBJ低、高剂量组在造模成功30 min后经尾静脉分别注射XBJ5、20 mL/kg,对照组及SAP模型组注射等体积生理盐水。24 h后,从上述4组中各随机抽取10只大鼠处死,留取腹水、胰腺、肺脏等组织样本;Evans blue法检测各组余下大鼠肺脏毛细血管的通透性。

1.2.2 收集大鼠腹水及组织干湿重比值测定 无菌术操作下,切开大鼠腹壁,用10 mL注射器收集腹水,于无菌量筒中测量腹液体积并记录;取部分新鲜胰腺、肺组织样本称重得其湿质量为m₁、m₂,将上述样本置于56℃烘干箱烘干24 h后称重,分别对应的组织样本干质量为m₃、m₄,m₃/m₁或m₄/m₂分别

为胰腺、肺组织样本的干湿重比值。

1.2.3 酶联免疫吸附法(ELISA)测定腹水淀粉酶含量 用3 000 r/min 离心20 min 取腹水上清, 取10 μL 待测液加入酶标板稀释至50 μL, 封板膜封闭后37℃温育30 min 后洗涤, 加入50 μL 酶标试剂重复温育后洗涤, 加入显色剂A、B各50 μL 显色, 15 min 后加入50 μL 终止液终止显色, 酶标仪测定450 nm 波长下吸光度, 根据淀粉酶试剂盒说明书配置标准品并绘制相关标准曲线, 计算各组腹水淀粉酶含量。

1.2.4 苏木精-伊红(HE)染色及病理评分 取部分胰尾、右侧下叶肺组织, 经4%多聚甲醛固定48 h 后, 在75%酒精中脱水1 h、80%酒精中脱水1 h、95%酒精中脱水2 h、100%酒精中脱水5 h, 经二甲苯透明3次, 每次10 min, 用56~58℃融化的石蜡包埋组织, 冷却后用自动切片机切取4.5 μm 切片, 60℃烤片30 min 后37℃烘箱过夜, 经二甲苯及梯度酒精脱蜡、脱水后, 苏木素染色4.5 min、伊红染色2 min, 经蒸馏水充分冲洗、二甲苯透明后, 应用中性树胶封片, 显微镜下观察各组织形态学改变, 依据Schmidt病理评分标准进行评分。

1.2.5 Western印迹检测相关蛋白表达 各组均取约5 g 肺组织, 经RIPA裂解液裂解后使用超声仪匀浆提取总蛋白, 通过BCA蛋白检测试剂盒测定蛋白浓度, 经loading buffer配平后, 以GAPDH(1:1 000)为内参, 各上样液经SDS-PAGE凝胶电泳分离、转膜、封闭, 孵育一抗Anti-ROCK1抗体(1:500)、Anti-MYPT1抗体(1:500)、Anti-pMLC抗体(1:1 000), 4℃过夜后经TBST震荡洗涤3次, 孵育山羊抗鼠IgG-HRP(1:5 000)二抗1 h, TBST震荡洗涤3次加入ECL发光显影, 目标蛋白条带图像后经Image J 处理进行比较。

1.2.6 Evans blue法检测肺毛细血管通透性 SAP造模成功24 h 后, 经大鼠尾静脉注射2%Evans blue无菌溶液0.25 mL/100 mg 大鼠体重, 30 min 后快速处死大鼠, 无菌术解剖胸腔, 留取肺组织样本, 经56℃烘干箱烘干, 取适量组织加入甲酰胺溶液0.5 mL/(50~100) mg 标本, 55℃水浴24 h 提取组织中Evans blue, 测量溶液620 nm 处吸光度值, 通过绘制浓度-吸光度标准曲线进行计算单位质量肺组织中Evans blue含量, Evans blue渗出量代表肺毛细血管通透性^[17]。

1.3 统计学处理 采用SPSS 25.0进行统计学分析, 正态分布的计量数据用 $\bar{x}\pm s$ 表示, 两组间比较采用两独立样本t检验, 3组间比较采用单因素方差分析, 所有检验均为双侧, $P<0.05$ 为差异有统计学意义。

2 结果

2.1 腹水量及腹水淀粉酶含量比较 与对照组相比, SAP模型组腹水量、腹水淀粉酶含量明显升高($t=-21.73$ 、 -40.72 , 均 $P<0.01$); SAP模型组、XBJ低剂量组、XBJ高剂量组的腹水量、腹水淀粉酶含量均逐渐降低($F=39.66$ 、 141.78 , 均 $P<0.01$), 见表1。

表1 腹水量及腹水淀粉酶含量比较($n=10$, $\bar{x}\pm s$)

Tab.1 Comparison of the water volume and amylase content of ascites($n=10$, $\bar{x}\pm s$)

组别	腹水量(mL)	腹水淀粉酶含量(U/dL)
对照组	0.19±0.02	2 986.20±151.40
SAP模型组	6.79±0.96 ^a	15 212.20±937.40 ^a
XBJ低剂量组	5.25±0.37	13 263.50±748.40
XBJ高剂量组	4.12±0.55	9 117.00±782.10
<i>F</i>	39.66	141.78
<i>P</i>	<0.01	<0.01

注:SAP:重症急性胰腺炎; XBJ: 血必净; 与对照组相比, ^a $P<0.01$

2.2 组织干湿重比值的测定及肺组织Evans blue渗出量的比较 与对照组相比, SAP模型组胰腺干湿重比值、肺脏干湿重比值明显降低($t=19.83$ 、 15.47 , 均 $P<0.01$), 肺组织中Evans blue渗出量明显升高($t=-27.9$, $P<0.01$)。SAP模型组、XBJ低剂量组、XBJ高剂量组胰腺干湿重比值、肺脏干湿重比值逐渐升高($F=75.19$ 、 15.47 , 均 $P<0.01$); 肺组织中Evans blue渗出量逐渐降低($F=99.52$, $P<0.01$), 见表2。

表2 干湿重比值测定及肺组织Evans blue渗出量比较($n=10$, $\bar{x}\pm s$)

Tab.2 Determination of dry-wet weight ratio and comparison of Evans blue exudation in lung tissue($n=10$, $\bar{x}\pm s$)

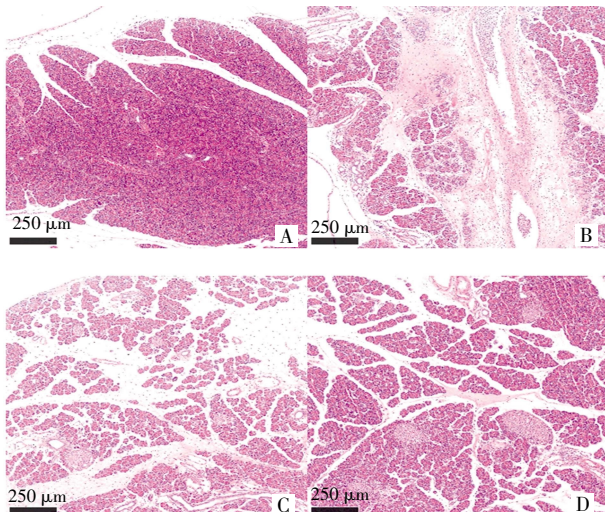
组别	胰腺干湿重比($\times 10^{-3}$)	肺脏干湿重比($\times 10^{-3}$)	肺组织Evans blue定量(ng EB/mg tissue)
对照组	3.43±0.19	3.34±0.20	0.23±0.05
SAP模型组	2.04±0.11 ^a	1.91±0.27 ^a	0.82±0.04 ^a
XBJ低剂量组	2.38±0.13	2.30±0.10	0.69±0.04
XBJ高剂量组	2.67±0.10	2.72±0.14	0.49±0.07
<i>F</i>	75.19	15.47	99.52
<i>P</i>	<0.01	<0.01	<0.01

注:SAP:重症急性胰腺炎; XBJ: 血必净; 与对照组相比, ^a $P<0.01$

2.3 HE染色及病理评分

2.3.1 胰腺组织HE染色及病理评分 对照组大鼠胰腺组织结构完整, 腺泡细胞排列规则, 导管形态自然, 血管连续性完好, 未见炎性细胞大量浸润; SAP模型组大鼠胰腺腺泡结构弥漫性破坏, 大片腺泡细胞融合坏死、脂肪组织溶解, 间质毛细血管连续性破坏伴红细胞游离, 大量中性粒细胞及单核巨噬细胞、淋巴细胞浸润; XBJ低剂量组病变较SAP模型组减轻, 可见腺泡细胞片状坏死、脂肪组织溶解, 毛细血管连续性破坏伴大量炎性细胞浸润, 可

见散在胰岛,结构欠规整;XBJ高剂量组大鼠胰腺腺泡细胞呈点状坏死,小叶形态结构较为完整,散在胰岛结构完整,未见明显出血及炎性细胞浸润,见图1。依据Schmidt标准进行病理评分发现,SAP模型组较对照组大鼠胰腺病理得分明显增加($t=-42.79$, $P<0.01$);SAP模型组、XBJ低剂量组、XBJ高剂量组的大鼠胰腺病理得分逐渐降低($F=175.43$, $P<0.01$),见表3。



注:SAP:重症急性胰腺炎;XBJ:血必净;A:对照组;B:SAP模型组;C:XBJ低剂量;D:XBJ高剂量

图1 胰腺组织HE染色结果(100×)

Fig.1 HE staining results of pancreatic tissue(100×)

2.3.2 肺组织HE染色及病理评分 如图2所示,对照组大鼠肺小叶各级气道如呼吸性细支气管、肺泡管及肺泡结构清晰、完整,肺泡腔内无渗出,肺泡隔内毛细血管完整,内皮细胞排列紧密,血管内壁光滑,间质内可见少量游离巨噬细胞;SAP模型组大鼠终末气道结构紊乱,呼吸性细支气管、肺泡管和肺泡内大量炎性渗出,肺间隔弥漫性增厚,间质内可见大量游离红细胞、中性粒细胞,毛细血管高度扩张、充血,小血管内可见透明血栓形成;XBJ低剂量组大鼠肺泡间隔增厚程度较SAP模型组降低,游离红细胞减少;XBJ高剂量组大鼠肺间隔较SAP模型组明显变窄,终末气道包括肺泡腔内渗出明显减少。依据Schmidt标准进行肺组织病理评分发现,SAP模型组较对照组肺组织病理得分明显升高($t=-37.57$, $P<0.01$);SAP模型组、XBJ低剂量组、XBJ高剂量组肺组织病理得分逐渐降低($F=126.00$, $P<0.01$),见表3。

2.3 肺组织中 ROCK1-MYPT1-pMLC表达分析 如图3所示,SAP模型组较对照组肺组织中ROCK1、pMLC蛋白表达量明显升高($t=-16.97$ 、 -13.53 ,均 $P<$

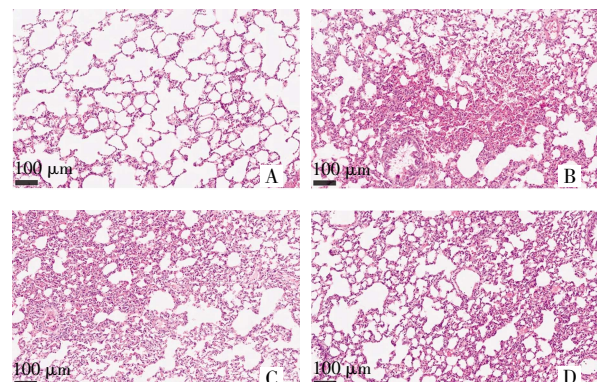
0.01),MYPT1表达量显著降低($t=23.30$, $P<0.01$);SAP模型组、XBJ低剂量组、XBJ高剂量组肺组织中ROCK1、pMLC蛋白表达量逐渐降低($F=84.89$ 、 50.84 ,均 $P<0.01$),MYPT1表达量显著升高($F=48.68$, $P<0.01$)。

表3 胰腺及肺组织病理评分比较($n=10$, $\bar{x}\pm s$)

Tab.3 Comparison of pathological scores of pancreases and lung ($n=10$, $\bar{x}\pm s$)

组别	胰腺组织病理评分	肺组织病理评分
对照组	0.28±0.18	0.50±0.20
SAP模型组	13.45±0.96 ^a	10.50±0.82 ^a
XBJ低剂量组	10.15±0.88	7.90±0.94
XBJ高剂量组	6.40±0.66	4.50±0.78
F	175.43	126.00
P	<0.01	<0.01

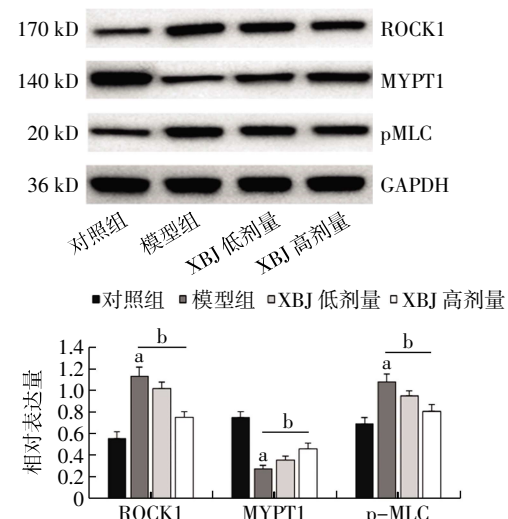
注:SAP:重症急性胰腺炎;XBJ:血必净;与对照组相比,^a $P<0.01$



注:SAP:重症急性胰腺炎;XBJ:血必净;A:对照组;B:SAP模型组;C:XBJ低剂量;D:XBJ高剂量

图2 肺组织HE染色结果(200×)

Fig.2 HE staining results of lung tissue(200×)



注:SAP:重症急性胰腺炎;XBJ:血必净;与对照组相比,^a $P<0.01$;SAP模型组、XBJ低剂量、XBJ高剂量相比,^b $P<0.01$

图3 肺组织中ROCK1、MYPT1、pMLC的表达

Fig.3 Expression of ROCK1,MYPT1 and pMLC in lung tissue

3 讨论

肺泡毛细血管高通透性是 SAP 肺损伤的主要特征之一^[9],由于 SAP 内环境严重紊乱,内皮细胞代谢功能障碍,引发细胞间隙增宽、血液成分渗漏,导致肺间质水肿、气体弥散障碍、通气血流比例失调而进展成 ALI/ARDS^[4-8]。Evans blue 可以与血液中白蛋白紧密结合,当毛细血管通透性增高导致白蛋白渗出时组织间质中 Evans blue 含量可随之升高,组织中 Evans blue 含量可代表毛细血管通透性状态^[17]。本实验应用 4.5% 牛磺胆酸钠经大鼠胰胆管逆行注射 24 h 后发现,SAP 模型组大鼠呼吸急促,腹水量、腹水淀粉酶含量显著升高,胰腺高度水肿伴出血、坏死,肺脏水肿、组织中 Evans blue 含量明显升高,胰腺及肺组织病理评分显著升高,说明 SAP 肺损伤大鼠模型构建成功。本课题组前期在应用相同方法构建的 SAP 大鼠模型中发现,外周血中线粒体 DNA (mtDNA)、N-甲酰肽(NFPs)等损伤相关的分子模式(DAMPs)以及髓过氧化物酶(MPO)、肿瘤坏死因子(TNF)- α 、白细胞介素(IL)-1、IL-6 等多种细胞因子含量升高,胰腺及肺组织高表达甲酰肽受体 1(FPR1),并且其升高程度与 SAP 脏器水肿及器官功能障碍呈正相关^[16,18-19]。受益于 Wenceslau 等^[20]提出 DAMPs 作用于 FPR1 引发胞内 RhoA/ROCK/CDC42 信号通路激活使内皮细胞收缩、细胞间隙增大、组织水肿的启发,课题组推测 ROCK1-MYPT1-pMLC 信号通路参与的细胞骨架变构、细胞收缩等生理过程参与了 SAP 肺损伤的形成,XBJ 可能的治疗机制与降低 DAMPs 及细胞因子释放并作用于内皮细胞该信号通路有关。

相关实验研究表明,ROCK1 信号通路参与调节内皮细胞收缩导致的毛细血管渗漏。YE 等^[21]通过检测人脐静脉内皮细胞(HUVECs)中 RhoA、ROCK 蛋白水平以及细胞紧密连接蛋白如闭锁小带蛋白 1(ZO-1)、闭塞蛋白发现,TNF- α 上调了 RhoA 和 ROCK 的表达,使李斯特菌感染后的 HUVECs 中 ZO-1 和闭塞蛋白表达降低,促进内皮细胞骨架重排及血管高通透性的发生。YANG 等^[22]发现,应用 ROCK1 活性抑制剂 Y-27632 可显著抑制 TNF- α 诱导的 HUVECs 凋亡并保持血管内皮的完整性。赵宏等^[23]发现病理因素高糖可刺激肾脏毛细血管内皮细胞 ROCK1 活化,通过提高 MLC 磷酸化下调缝隙连接蛋白 43 的表达,使白蛋白渗漏、加速肾小球的损伤。MYPT1 是肌球蛋白轻链磷酸酶的活性亚基,其表达升高可维持病理性内皮细胞的收缩^[24]。FU 等^[25]通过检测 ROCK、MYPT1 和 VE-cadherin 的表

达及 F-肌动蛋白的分布和形态论证了 TNF- α /RhoA/ROCK 信号通路参与血管内皮细胞高通透性的结论。本研究发现 SAP 肺损伤大鼠模型中肺组织 ROCK1、pMLC 表达增加、MYPT1 表达降低,推测高表达的 DAMPs 及炎症因子参与了该信号通路的激活,其引发的内皮细胞骨架重构、紧密连接蛋白减少、细胞间隙增宽等是造成肺水肿及出现 ALI/ARDS 的原因。

XBJ 是我国中西医结合危重症医学领域开拓者王今达教授根据清代医家王清任的血府逐瘀方化载而来,由君药红花及丹参活血祛瘀止痛、臣药川芎和赤芍活血祛瘀、佐药当归养血益阴合用而成,为治疗温热类疾病之良方。多项动物实验及大规模临床试验研究发现 XBJ 在多种诱因引发的 SIRS、ALI/ARDS、MODS 治疗中效果确切,尤其在 2019 新冠肺炎疫情防控中扮演了重要作用^[13-16]。本研究发现,应用 XBJ 低剂量及高剂量干预 SAP 大鼠后,大鼠生命体征、腹水渗出、器官水肿、肺泡毛细血管高通透性及病理改变等指标逐渐改善;同时 XBJ 剂量依赖性地降低了肺组织 ROCK1、pMLC 的表达,提高了 MYPT1 表达,体现了 XBJ 对 SAP 肺损伤良好的治疗作用,并间接证实 XBJ 参与了肺组织细胞 ROCK1-MYPT1-pMLC 信号通路表达的调节,这可能是 XBJ 治疗 SAP 肺损伤的一种机制。

当代药学大家刘昌孝院士提出了“物质-药代-功效”关联的现代中药创新研发思路^[26]。在基于 XBJ 质量标志物的相关研究发现,羟基红花黄色素 A(HSYA)、丹酚酸 B(Sal B)、芍药苷、洋川芎内酯等化合物含量与 XBJ 药效质量密切相关^[27]。实验研究发现 HSYA 通过抑制 TLR4/NF- κ B/NLRP3 通路,减少血管紧张素Ⅱ诱导的血管外膜成纤维细胞的迁移^[28],同时通过 TRPV4 依赖性 Ca²⁺的流入、增加血管内皮细胞 NO 的合成,实现大鼠肠系膜动脉扩张、减少内皮细胞凋亡的作用^[29];Sal B 具有抗氧化应激、诱导细胞自噬、抑制内质网应激、抑制内皮炎症和黏附分子表达、抑制内皮细胞通透性及抗血栓形成的作用^[30];芍药苷是一种单萜类糖苷化合物,可抑制机体 TNF- α 、IL-1、IL-6 等多种炎症因子释放、减少 NF- κ B 的表达,发挥抗炎、扩血管及解热解痉的作用^[31-32];洋川芎内酯类化合物可能包括对 Toll 样受体 4/NF- κ B、细胞外信号调节激酶、p38 丝裂原活化蛋白激酶和 c-Jun 氨基末端激酶等多条信号通路的调控作用,发挥抗炎、抗菌、抗纤维化及心血管保护的作用^[33]。但值得注意的是,XBJ 的治疗机制是中药复杂配伍环境下多种药效分子相互作用、相互较

衡的整体结果,单一药物分子及靶点尚不能阐明其实际作用机制。在未来 XBJ 药理机制的研究中,基于中医药辨证论治理论指导下,应用现代网络药理学进行多靶点、多分子对接并于细胞、动物等层面验证的方法,对详细阐明 XBJ 治疗 SAP 肺损伤机制具有创新及推动意义。

综上,ROCK1-MYPT1-pMLC 信号通路激活引发的内皮细胞骨架重构、紧密连接蛋白减少、细胞间隙增宽等是 SAP 肺损伤的成因;XBJ 通过降低多种细胞因子及 DAMPs 形成,抑制 ROCK1-MYPT1-pMLC 信号通路活化,对 SAP 肺损伤起到了治疗作用。

参考文献:

- [1] 中华医学会外科学分会胰腺外科学组. 中国急性胰腺炎诊治指南(2021)[J].浙江实用医学,2021,26(6):511-519,535.
- [2] PEERY A F,CROCKETT S D,MURPHY C C,et al. Burden and cost of gastrointestinal,liver, and pancreatic diseases in the United States:update 2021[J]. Gastroenterology,2022,162(2):621-644.
- [3] WILEY M B,MEHROTRA K,BAUER J,et al. Acute pancreatitis: current clinical approaches,molecular pathophysiology, and potential therapeutics[J]. Pancreas,2023,52(6):e335-e343.
- [4] ZHANG Q,RAOOF M,CHEN Y,et al. Circulating mitochondrial DAMPs cause inflammatory responses to injury[J]. Nature,2010, 464(7285):104-107.
- [5] WANG Z,LIU J,WANG Y,et al. Identification of key biomarkers associated with immunogenic cell death and their regulatory mechanisms in severe acute pancreatitis based on WGCNA and machine learning[J]. Int J Mol Sci,2023,24(3):3033.
- [6] SHAH J,RANA S S. Acute respiratory distress syndrome in acute pancreatitis[J]. Indian J Gastroenterol,2020,39(2):123-132.
- [7] STERNBY H,HARTMAN H,THORLACIUS H,et al. The initial course of IL-1 β ,IL-6,IL-8,IL-10,IL-12,IFN- γ and TNF- α with regard to severity grade in acute pancreatitis[J]. Biomolecules, 2021,11(4):591.
- [8] MEYER N J,GATTINONI L,CALFEE C S. Acute respiratory distress syndrome[J]. Lancet,2021,398(10300):622-637.
- [9] ZHOU J,ZHOU P,ZHANG Y,et al. Signal pathways and markers involved in acute lung injury induced by acute pancreatitis [J]. Dis Markers,2021,21(3):9947.
- [10] GOECKELER Z M,WYSOMERSKI R B. Myosin light chain kinase-regulated endothelial cell contraction:the relationship between isometric tension,actin polymerization, and myosin phosphorylation[J]. J Cell Biol,1995,130(3):613-627.
- [11] ZHAO L,HU J,ZHENG P,et al. PAR1 regulates sepsis-induced vascular endothelial barrier dysfunction by mediating ERM phosphorylation via the RhoA/ROCK signaling pathway[J]. Int Immunopharmacol,2023,124:110992.
- [12] WANG T,KANG W,DU L,et al. Rho-kinase inhibitor Y-27632 facilitates the proliferation,migration and pluripotency of human periodontal ligament stem cells[J]. J Cell Mol Med,2017,21:3100-3112.
- [13] CHEN Y,TONG H,PAN Z,et al. Xuebijing injection attenuates pulmonary injury by reducing oxidative stress and proinflammatory damage in rats with heat stroke[J]. Exp Ther Med,2017,13(6): 3408-3416.
- [14] LUO Z,CHEN W,XIANG M,et al. The preventive effect of Xuebijing injection against cytokine storm for severe patients with COVID-19:a prospective randomized controlled trial[J]. Eur J Integr Med,2021,42:101305.
- [15] SONG Y,Yao C,YAO Y,et al. Xuebijing injection versus placebo for critically ill patients with severe community-acquired pneumonia :arandomized controlled trial[J]. Crit Care Med,2019,47(9): e735-e743.
- [16] 肖懿,冯志乔,张桂贤,等.血必净注射液调节线粒体 N-甲酰肽/NLRP3 炎症通路对重症急性胰腺炎大鼠模型的治疗机制[J].中国实验方剂学杂志,2022,28(7):88-94.
- [17] RADU M,CHERNOFF J. An *in vivo* assay to test blood vessel permeability[J]. J Vis Exp,2013,(73):e50062.
- [18] 胡炜.清胰汤调控 DAMPs 对 SAP-ALI 大鼠的治疗机制及对肠道微生态调整的初步探讨[D].天津医科大学,2020.
- [19] 肖懿,张桂贤,高瑞芳,等.重症急性胰腺炎大鼠血浆中 6 种线粒体 N-甲酰肽及胰腺 FPR1 的表达研究[J].天津医药,2022,50 (2):150-154.
- [20] WENCESLAU C F,MCCARTHY C G,WEBB RC. Formyl peptide receptor activation elicits endothelial cell contraction and vascular leakage[J]. Front Immunol,2016,7:297.
- [21] YE L,LIAN Z Y,YANG H,et al. TNF- α activates RhoA/ROCK signaling pathway and increases permeability of endothelial cells infected with Listeria monocytogenes [J]. Xi Bao Yu Fen Zi Mian Yi Xue Za Zhi,2020,36(3):193-197.
- [22] YANG L,TANG L,DAI F,et al. Raf-1/CK2 and RhoA/ROCK signaling promote TNF- α -mediated endothelial apoptosis via regulating vimentin cytoskeleton[J]. Toxicology,2017,389:74-84.
- [23] ZHAO H,KONG H,WANG W,et al. High glucose aggravates retinal endothelial cell dysfunction by activating the RhoA/ROCK1/pMLC/Connexin43 signaling pathway[J]. Invest Ophthalmol Vis Sci, 2022,63(8):22.
- [24] MACDONALD J A,WALSH M P. Regulation of smooth muscle myosin light chain phosphatase by multisite phosphorylation of the myosin targeting subunit,MYPT1[J]. Cardiovasc Hematol Disord Drug Targets,2018,18(1):4-13.
- [25] FU W,LIU S,LUO L,et al. Anti-inflammatory mechanism of ulinastatin:inhibiting the hyperpermeability of vascular endothelial cells induced by TNF- α via the RhoA/ROCK signal pathway [J]. Int Immunopharmacol,2017,46:220-227.
- [26] 刘昌孝,张铁军.基于“物质-药代-功效”关联的中药创新研发思路[J].中草药,2022,53(1):1-7.
- [27] 蔡楠,曹宁宁,赵利斌,等.基于“五原则”的血必净注射液质量标志物的预测分析[J].天津中医药,2021,38(8):1062-1070.
- [28] LIU L,CUI Q,SONG J,et al. Hydroxysafflower yellow A inhibits vascular adventitial fibroblast migration via NLRP3 inflammasome inhibition through autophagy activation[J]. Int J Mol Sci,2022,24 (1):172.

- [29] YANG J,WANG R,CHENG X,et al. The vascular dilatation induced by Hydroxysafflower yellow A (HSYA) on rat mesenteric artery through TRPV4 -dependent calcium influx in endothelial cells[J]. *J Ethnopharmacol*,2020,256:112790.
- [30] ZHAO Y,SHAO C,ZHOU H,et al. Salviaolic acid B inhibits atherosclerosis and TNF- α -induced inflammation by regulating NF- κ B/NLRP3 signaling pathway[J]. *Phytomedicine*,2023,119:155002.
- [31] 庞彬彬,陈震,邢怡桥.芍药苷调节 RhoA/ROCK 信号通路对实验性自身免疫性葡萄膜炎小鼠 Th17/Treg 免疫平衡的影响[J]. *中药新药与临床药理*,2024,35(4):506-512.
- [32] 张育贵,张淑娟,边甜甜,等.芍药苷药理作用研究新进展[J]. *中草药*,2019,50(15):3735-3740.
- [33] 李青泉,万建波,赵璐.洋川芎内酯类化合物药理活性研究进展[J].*针灸和草药(英文)*,2023,3(3):180-188.

(2024-03-13 收稿)

(上接第 409 页)

- dence and mortality worldwide:sources, methods and major patterns in GLOBOCAN 2012[J]. *Int J Cancer*,2015,136(5):E359-E386.
- [2] WANG G,LI J,BOJMAR L,et al. Tumour extracellular vesicles and particles induce liver metabolic dysfunction[J]. *Nature*,2023,618(7964):374-382.
- [3] BIAN X L,CHEN H Z,YANG P B,et al. Nur77 suppresses hepatocellular carcinoma via switching glucose metabolism toward gluconeogenesis through attenuating phosphoenolpyruvate carboxykinase sumoylation[J]. *Nat Commun*,2017,8:14420.
- [4] ROACH P J,DEPAOLI-ROACH A A,HURLEY T D,et al. Glycogen and its metabolism:some new developments and old themes[J]. *Biochem J*,2012,441(3):763-787.
- [5] BARENS P J,KAEIN M. Nuclear factor- κ B:a pivotal transcription factor in chronic inflammatory diseases[J]. *N Engl J Med*,1997,336(15):1066-1071.
- [6] KUO W Y,HWU L,WU C Y,et al. STAT3/NF- κ B-regulated lentiviral TK/GCV suicide gene therapy for cisplatin-resistant triple-negative breast cancer[J]. *Theranostics*,2017,7(3):647-663.
- [7] YU C,CHEN S,GUO Y,et al. Oncogenic TRIM31 confers gemcitabine resistance in pancreatic cancer via activating the NF- κ B signaling pathway[J]. *Theranostics*,2018,8(12):3224-3236.
- [8] YAO F,DENG Y,ZHAO Y,et al. A targetable LIFR-NF- κ B-LCN2 axis controls liver tumorigenesis and vulnerability to ferroptosis[J]. *Nat Commun*,2021,12(1):7333.
- [9] LIU J,WU Z,HAN D,et al. Mesencephalic astrocyte-derived neurotrophic factor inhibits liver cancer through small ubiquitin-related modifier (SUMO)ylation-related suppression of NF- κ B/snail signaling pathway and epithelial-mesenchymal transition[J]. *Hepatology*,2020,71(4):1262-1278.
- [10] ROUSSET M,ZWEIBAUM A,FOGH J. Presence of glycogen and growth-related variations in 58 cultured human tumor cell lines of various tissue origins[J]. *Cancer Res*,1981,41(3):1165-1170.
- [11] LEA M A,MURPHY P,MORRIS H P. Glycogen metabolism in regenerating liver and liver neoplasms[J]. *Cancer Res*,1972,32(1):61-66.
- [12] CHEN S L,HUANG Q S,HUANG Y H,et al. GYS1 induces glycogen accumulation and promotes tumor progression via the NF- κ B pathway in clear cell renal carcinoma[J]. *Theranostics*,2020,10(20):9186-9199.
- [13] HUANG Q,LI J,XING J,et al. CD147 promotes reprogramming of glucose metabolism and cell proliferation in HCC cells by inhibiting the p53-dependent signaling pathway[J]. *J Hepatol*,2014,61(4):859-866.
- [14] CHAO T,ZHOU X,CAO B,et al. Pleckstrin homology domain-containing protein PHLDB3 supports cancer growth via a negative feedback loop involving p53[J]. *Nat Commun*,2016,7:13755.
- [15] WAN F,ANDERSON D E,BARNITZ R A,et al. Ribosomal protein S3:a KH domain subunit in NF- κ B complexes that mediates selective gene regulation[J]. *Cell*,2007,131(5):927-939.
- [16] JIANG P,DU W,WANG X,et al. p53 regulates biosynthesis through direct inactivation of glucose-6-phosphate dehydrogenase[J]. *Nat Cell Biol*,2011,13(3):310-316.
- [17] MORANDY A,INDRACCOLO S. Linking metabolic reprogramming to therapy resistance in cancer[J]. *Biochim Biophys Acta Rev Cancer*,2017,1868(1):1-6.

(2024-03-19 收稿)